Bioorganic & Medicinal Chemistry 22 (2014) 6324–6332

Contents lists available at ScienceDirect

Bioorganic & Medicinal Chemistry

journal homepage: www.elsevier.com/locate/bmc

Novel strategy to boost oral anticoagulant activity of blood coagulation enzyme inhibitors based on biotransformation into hydrophilic conjugates

Tsukasa Ishihara [a,*], Yuji Koga [a], Kenichi Mori [a], Keizo Sugasawa [a], Yoshiyuki Iwatsuki [b], Fukushi Hirayama [a]

[a] Drug Discovery Research, Astellas Pharma Inc., 21, Miyukigaoka, Tsukuba-shi, Ibaraki 305-8585, Japan
[b] Pharmacovigilance, Astellas Pharma Inc., 2-5-1, Nihonbashi-Honcho, Chuo-ku, Tokyo 103-8411, Japan

ARTICLE INFO

Article history:
Received 1 September 2014
Revised 26 September 2014
Accepted 30 September 2014
Available online 19 October 2014

Keywords:
Factor Xa
Anticoagulant
Conjugation
Docking study

ABSTRACT

The blood coagulation cascade represents an attractive target for antithrombotic drug development, and recent studies have attempted to identify oral anticoagulants with inhibitory activity for enzymes in this cascade, with particular attention focused on thrombin and factor Xa (fXa) as typical targets. We previously described the discovery of the orally active fXa inhibitor darexaban (**1**) and reported a unique profile that compound **1** rapidly transformed into glucuronide YM-222714 (**2**) after oral administration. Here, we propose a novel strategy towards the discovery of an orally active anticoagulant that is based on the bioconversion of a non-amidine inhibitor into the corresponding conjugate to boost ex vivo anticoagulant activity via an increase in hydrophilicity. Computational molecular modeling was utilized to select a template scaffold and design a substitution point to install a potential functional group for conjugation. This strategy led to the identification of the phenol-derived fXa inhibitor ASP8102 (**14**), which demonstrated highly potent anticoagulant activity after biotransformation into the corresponding glucuronide (**16**) via oral dosing.

1. Introduction

Intravascular clot formation results in thromboembolic diseases including ischemic stroke, deep venous thrombosis, myocardial infarction, unstable angina, and pulmonary embolism, all of which are major causes of morbidity and mortality in the industrialized world. Enzymes in the blood coagulation cascade, such as thrombin and fXa, are attractive targets for the prevention of thrombosis, with numerous efforts devoted to the discovery of inhibitors against these enzymes that can act as orally active anticoagulant agents.

Approaches to the discovery of oral anticoagulant drugs that directly inhibit blood coagulation enzymes are classified into two categories. One involves approaches based on the strategy of amidine prodrugs, represented by the anticoagulants ximelagatran[1] and dabigatran etexilate.[2] An amidine prodrug is bioconverted into the corresponding amidine inhibitor after oral administration, and the amidine group forms a bidentate salt bridge interaction with the carboxylic acid of Asp189 in the S1 site of the enzyme. Although amidine-derived inhibitors demonstrate potent in vivo anticoagulant and antithrombotic activity due to their overall high hydrophilicity, associated with the inhibitor's highly polar amidine group, the hydrophilic and basic profile of the amidine moiety also causes a reduction in membrane permeability and oral bioavailability. Thus, the prodrug strategy seeks to mask the high hydrophilicity and basicity of the amidine unit to improve the inferior profile of amidine-derived inhibitors.

The other methodology involves nonamidine-type inhibitors—eliminating highly hydrophilic and basic amidine groups to improve the oral bioavailability of inhibitors.[3] These efforts have already led to the discovery of the launched coagulants rivaroxaban,[4] apixaban,[5] and edoxaban.[6] These nonamidine-type inhibitors possess a small lipophilic substituent, such as a methoxy or chloro group, which occupies the small hydrophobic pocket formed by the residues Ala190, Val213, and Tyr228 in the bottom of the S1 site of the enzyme, or a less polar surrogate for an amidine group, such as an aromatic amine or benzylamine. However, the removal of the amidine group causes an increase in the overall lipophilicity of the inhibitor, which often leads to a detrimental reduction in anticoagulant potency.[3] Thus, concerted efforts have been devoted to managing both anticoagulant activity and pharmacokinetics profile of orally active anticoagulants.

* Corresponding author. Tel.: +81 29 863 6713; fax: +81 29 854 1519.
E-mail address: tsukasa.ishihara@astellas.com (T. Ishihara).

http://dx.doi.org/10.1016/j.bmc.2014.09.059
0968-0896/

Here, we propose adoption of a third strategy in the discovery of blood coagulation enzyme inhibitors with boosted anticoagulant effects after oral administration, based on non-amidine inhibitors, via bioconversion to corresponding highly hydrophilic conjugates.

2. Strategy

Inhibitors of enzymes in the blood coagulation cascade target the venous and arterial vascular system, therefore their high distribution in the circulation is preferred. Such a property is consistent with a pharmacokinetic profile of low distribution volume, and a general method to decrease volume of distribution is to increase hydrophilicity of a compound.[7] Consequently, an inhibitor with increased hydrophilicity is expected to improve in vivo antithrombotic effect. This concept is consistent with the previous result that found the fXa inhibitor **3**, which contains a combination of highly hydrophilic amidine and carboxylic acid, displays 30-fold higher activity in an in vivo thrombosis model during continuous intravenous infusion despite its equipotency to the non-amidine fXa inhibitor **4** in an in vitro anticoagulant assay (Fig. 1).[8] Pinto et al. also reported the desirability of a pharmacokinetic profile with low distribution volume towards vascular-targeted agents in the discovery process of the launched fXa inhibitor apixaban.[5]

We developed the fXa inhibitor **1** to demonstrate potent anticoagulant effect after oral administration (Fig. 1).[9] Compound **1** was found to be rapidly metabolized when dosed orally, and the predominant metabolite detected in the plasma was the corresponding glucuronide **2**. A comparison of the lipophilicity of the compounds **1** and **2** found that the latter was much more hydrophilic (*c*log*P* values of 2.30 for compound **1** and −1.03 for compound **2**),[10] which led us to consider whether compound **1**'s oral anticoagulant activity was achieved by it being converted into the highly hydrophilic glucuronide **2** in vivo. Biotransformation of a lipophilic amidine prodrug with high membrane permeability into a corresponding hydrophilic amidine inhibitor with high anticoagulant potency is the established methodology for identification of orally active anticoagulants.[1,2] Using this idea as a model, we investigated whether the biotransformation of a lipophilic precursor into the corresponding hydrophilic conjugate could be a new strategy for discovery of oral anticoagulants.

A key step for this strategy is the installation of a 'trigger' at an appropriate position of a suitable chemical scaffold. The trigger refers to a functional group with a potential to act as a substrate for conjugation. A phenolic hydroxyl group is preferable for the trigger owing to two reasons: conjugates of hydroxyl groups are known to be relatively stable compared to those of acyl or amino groups, and phenolic hydroxyl groups have less oxidizability than alcoholic hydroxyl groups. Similar to compound **1**, the launched phenol-derived cholesterol absorption inhibitor ezetimibe was found to rapidly undergo glucuronide conjugation before entering portal plasma via oral dosing.[11] This property indicates a general feature that phenolic hydroxyl groups can be precursors of highly hydrophilic glucuronide conjugates after oral administration.

Computational molecular modeling simulations could be utilized to identify an appropriate scaffold and where to install the triggering phenolic hydroxyl group. Figure 2 shows a proposed binding model of compound **1** and its glucuronide **2** to the active site of fXa. The sugar residue of compound **2** extends into solvent space without disturbing the interaction between the ligand and the enzyme, resulting in fXa inhibitory activity. A novel inhibitor can therefore be designed using computational molecular modeling by selecting a chemical scaffold on which a phenolic hydroxyl group is directed out of the binding site and into the bulk solvent. At the time our study was initiated,[12] only three representative scaffolds, compounds **5** (DPC423),[13] **6**,[14] and **7**,[15] had been reported as non-amidine fXa inhibitors (Fig. 1). Our computational modeling simulation of these three inhibitors and consideration of reactivity for glucuronidation led us to presume the followings:

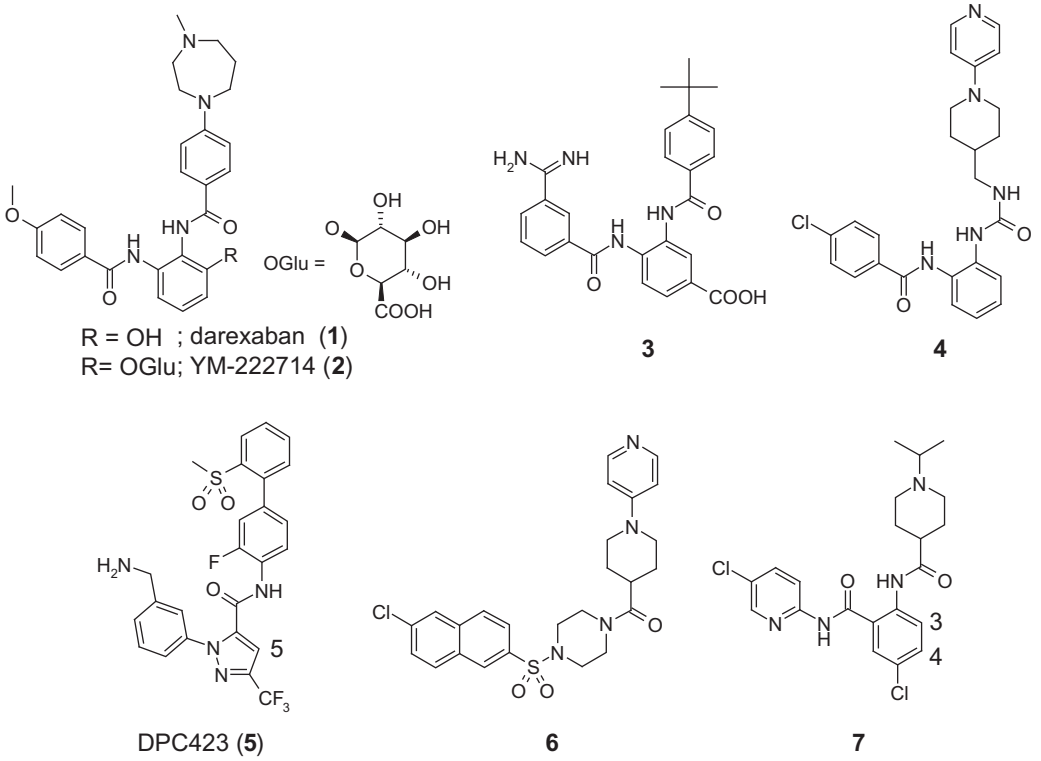

Figure 1. Structures of direct fXa inhibitors.

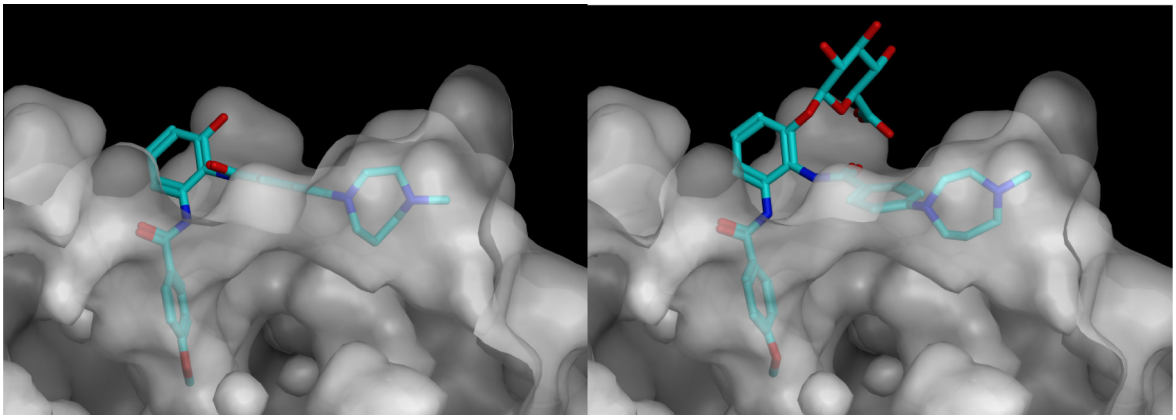

Figure 2. Docking model of compound **1** and glucuronide **2** complexed with the active site of factor Xa. Carbon atoms of compounds are colored cyan, while the protein surface is colored white.

Compound **5**: The aminomethylphenyl moiety was bound to ASP189 at the bottom of the S1 pocket and the biphenyl part lay deep within the S4 binding cleft. Therefore, both aromatic units were directed away from the bulk solvent (Fig. 3). Although the 5-position of the central pyrazole ring was oriented towards the solvent-exposed region, installation of a hydroxyl group onto this position would be inadequate, because 2,6-disubstituted aromatic rings are very poor substrates for glucuronidation.[16]
Compound **6**: The naphthalene and pyridine rings deeply occupied the S1 and S4 binding cavities, respectively. All aromatic cores were shielded by the residues of these pockets and did not extend into the bulk solvent (Fig. 4).
Compound **7**: Although the distal pyridine ring was buried in the S1 pocket and made no contact with the aqueous environment surrounding the enzyme, the 3- and 4-positions on the central phenyl motif were oriented into the solvent region (Fig. 5). Reports revealed that 2-acetylaminophenol possesses greater reactivity than 3-acetylaminophenols and that 4-hydroxybenzamide is a poor substrate for glucuronidation.[16] These investigations led us to select the compound **7** as our template and introduce a trigger hydroxyl group onto the 3-position of its central phenyl ring.

3. Chemistry

Scheme 1 depicts the subsequent steps that were employed to elaborate the target compounds **13**–**16**. The starting material, 3-benzyloxy-2-nitrobenzoic acid (**8**),[17] was converted to acid chloride by treatment with oxalyl chloride and then coupled with 2-amino-5-chloropyridine to afford N^1-(2-pyridyl)anthranilamide **9**. Compound **9** was transformed to aminophenol **10** via a two-step sequence involving trifluoroacetic acid (TFA)-mediated deprotection of benzyl moiety followed by catalytic hydrogenation in the presence of Raney® nickel. Treatment of aminophenol **10** with

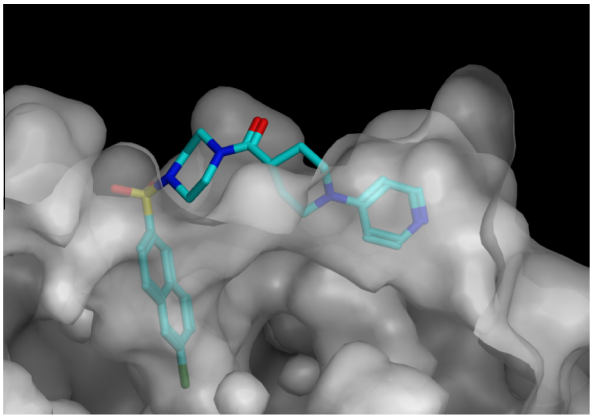

Figure 4. Docking model of compound **6** complexed with the active site of factor Xa. Carbon atoms of compounds are colored cyan, while the protein surface is colored white.

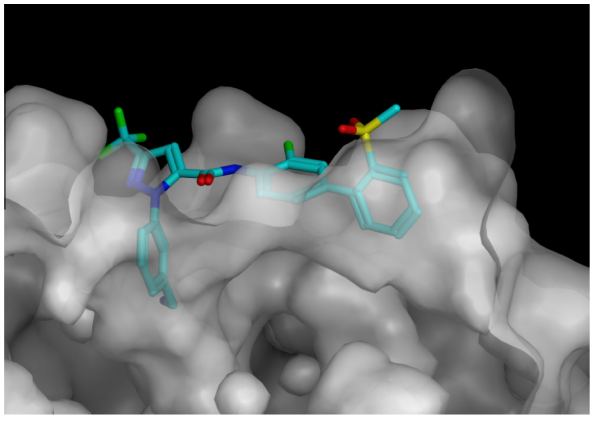

Figure 3. Docking model of compound **5** complexed with the active site of factor Xa. Carbon atoms of compounds are colored cyan, while the protein surface is colored white.

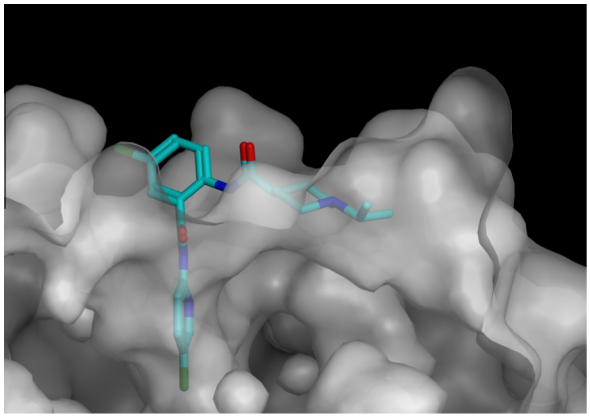

Figure 5. Docking model of compound **7** complexed with the active site of factor Xa. Carbon atoms of compounds are colored cyan, while the protein surface is colored white.

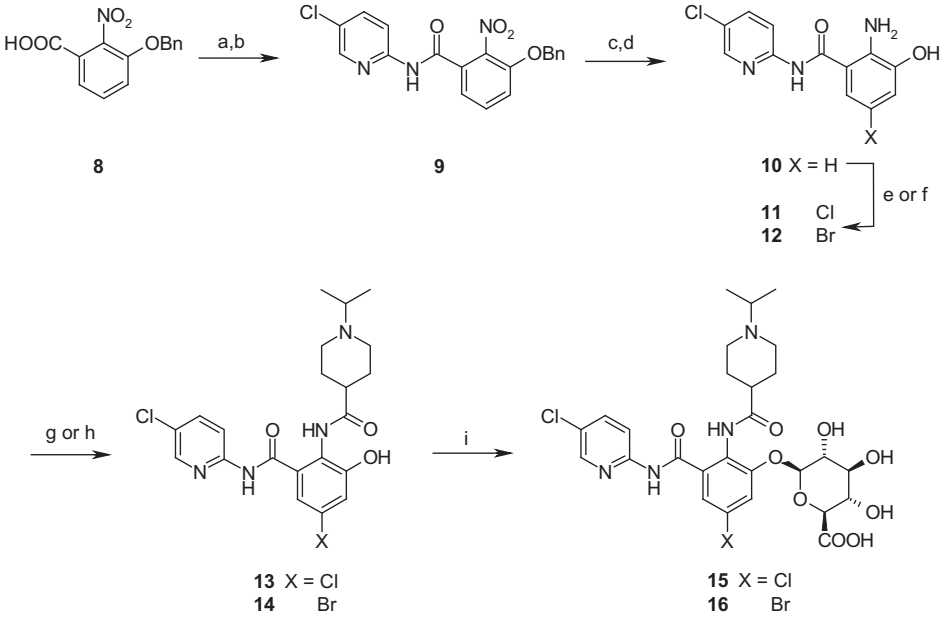

Scheme 1. Synthesis of Phenol–Derived Inhibitors and their Glucuronide Conjugates. Reagents and conditions: (a) $SOCl_2$, cat. *N*,*N*-dimethylformamide (DMF), ethyl acetate, 50 °C; (b) 2-amino-5-chloropyridine, pyridine, CH_3CN; (c) pentamethylbenzene, TFA, 40 °C; (d) H_2 (1 kgf/cm^2), Raney®-Ni, ethanol; (e) *N*-chlorosuccinimide, DMF, 50 °C; (f) *N*-bromosuccinimide, DMF, −15 °C; (g) 1-isopropylpiperidine-4-carboxylic acid (**17**), 1-hydroxybenzotriazole, 1-(3-dimethylaminopropyl)-3-ethylcarbodiimide hydrochloride, DMF; (h) 1-isopropylpiperidine-4-carboxylic acid, $SOCl_2$, cat. DMF, pyridine; (i) i. acetobromo-α-D-glucuronic acid methyl ester, 1,8-diazabicyclo-[5.4.0]-7-undecene, $CHCl_3$, methanol; ii. Na_2CO_3, H_2O.

N-chlorosuccinimide and *N*-bromosuccinimide gave 5-halo analogues **11** and **12**, respectively, which were then transformed into the N^2-acylanthranilamides **13** and **14**, respectively. Glycosylation of phenol derivatives **13** and **14** with acetobromo-α-D-glucuronic acid methyl ester in the presence of 1,8-diazabicyclo-[5.4.0]-7-undecene followed by basic hydrolysis gave the desired β-glucuronides **15** and **16**, respectively. A ^{1}H nuclear magnetic resonance (NMR) spectrum of compound **15** showed a signal at δ = 5.12 ppm with an axial–axial coupling of 6.8 Hz in agreement with its β-configuration of the anomeric position.[18] The structure of the β-configuration of compound **16** was also supported by an anomeric doublet at δ = 5.12 ppm with a coupling of 6.9 Hz characteristics of the expected axial–axial arrangement.

4. Results and discussion

Table 1 shows fXa inhibitory activity of phenol derivatives and the corresponding glucuronide conjugates **13**–**16**. As our molecular modeling study suggested that substitution onto the 3-position of the central phenyl ring would not interrupt binding with the enzyme due to the location towards the solvent–exposed region, none of investigated substituents resulted in any detrimental effects on inhibitor affinity. Although chlorinated phenol **13** and its glucuronide **15** demonstrated slightly less inhibitory activity against fXa than the deshydroxy parent compound **7**, the brominated phenol **14** and the corresponding glucuronide **16** displayed potent activity comparable to compound **7**. We therefore focused our attention to the brominated pair **14** and **16**. The phenol **14** and the corresponding glucuronide **16** displayed a potent inhibitory activity against fXa that was comparable to the deshydroxy analogue **7**. Confirmatory tests of compounds **14** and **16** revealed that both inhibitors demonstrated an in vitro PT-prolongation effect with CT_2 values of 0.31 and 0.28 μM, respectively. Subsequent screening against human thrombin for selectivity within the coagulation cascade and human trypsin for general specificity against serine proteases was carried out, and both compounds were found to be highly selective fXa inhibitors for these enzymes. Examination of physicochemical property indicated that the phenol **14** showed comparable membrane permeability to compound **7**.

The phenol **14** and its glucuronide **16** were subjected to further biological evaluation. Examination of anticoagulant effects via intravenous bolus injection revealed that the glucuronide **16** exhibited superior potency compared to the deshydroxy analogue **7** at about one-tenth the dose (Fig. 6). Compound **16** was 800-fold more hydrophilic compared to compound **7** (measured log$D_{7.4}$ values of 1.8 for compound **7** and −1.1 for compound **16**), which is consistent with our hypothesis that a highly hydrophilic profile is preferable for a blood coagulation enzyme inhibitor when targeting the vascular system and that a highly hydrophilic conjugated inhibitor will demonstrate potent ex vivo anticoagulant effect.

To examine pharmacokinetic profile, the phenol **14** was administered orally, and the plasma levels of this compound and the corresponding glucuronide **16** were monitored over time (Fig. 7). Phenol **14** was smoothly bioconverted into the glucuronide conjugate **16**, as markedly high concentrations of compound **16** were detected in plasma while both compound **14** and the corresponding sulfate conjugate were below the limit of quantification (10 ng/mL). Figure 8 displays the anticoagulant activity in cynomolgus monkeys after oral administration of the phenol **14** and the deshydroxy analogue **7**. Compound **14** showed an order of magnitude more effective than compound **7** in this assay. These results indicated that the phenolic hydroxyl group on compound **14** was subjected to rapid glucuronide-conjugation after oral dosing and that the resultant conjugate efficiently demonstrated potent *ex vivo* anticoagulant activity.

5. Conclusion

In this report, we propose a novel methodology for discovery of orally active inhibitors of the blood coagulation enzymes, which is based on biotransformation of non-amidine inhibitors into more hydrophilic conjugates. For the discovery of fXa inhibitors, we designed the phenol derivative **14** by selecting a template scaffold

Table 1
In vitro enzyme inhibitory activity, anticoagulant activity, and physicochemical property

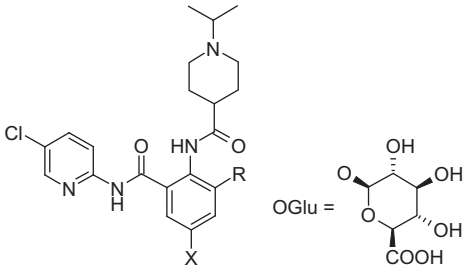

Compd	X	R	IC_{50}[a] (μM)			CT_2[b] (μM) PT[c]	PAMPA[d] (10^{-6} cm/s)
			fXa	Thrombin	Trypsin		
7	Cl	H	0.0058	NT[e]	NT[e]	0.22	>30
13	Cl	OH	0.0082	NT[e]	NT[e]	NT[e]	NT[e]
15	Cl	OGlu	0.015	NT[e]	NT[e]	NT[e]	NT[e]
14	Br	OH	0.0040	>100	>100	0.31	>30
16	Br	OGlu	0.0049	>100	>100	0.28	NT[e]

[a] Inhibitory activity against human purified enzymes. IC_{50} value are represented by the average of three separate determinations with an average standard error of the mean of <20%.
[b] CT_2 values are defined as the concentration required to double clotting time and represent the average of three separate determinations, with the average standard errors of the mean being <10%.
[c] Prothrombin time using cynomolgus monkey plasma.
[d] *p*ION membrane lipid was used at donor buffer, pH 6.5 (n = 2).
[e] Not tested.

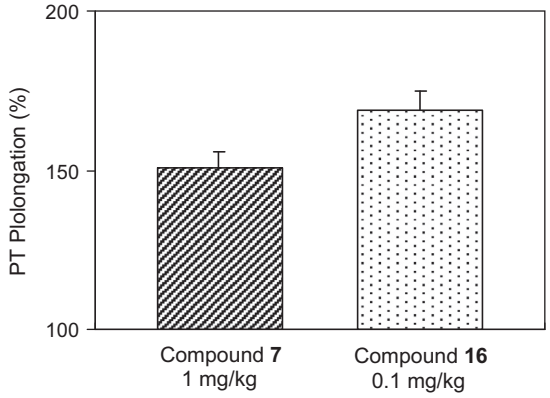

Figure 6. Anticoagulant activity of compounds **7** and **16** after intravenous bolus injection in cynomolgus monkeys. Relative prothrombin time (PT) compared to that measured using normal cynomolgus monkey plasma at 5 min after single intravenous bolus dosing (mean + standard deviation, n = 3).

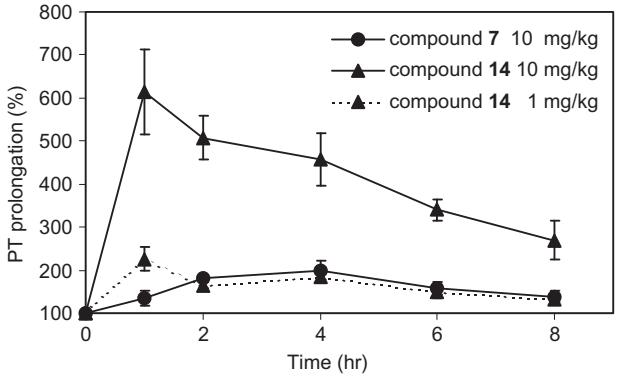

Figure 8. Anticoagulant activity in cynomolgus monkeys after oral administration of compounds **7** and **14**. Relative prothrombin time (PT) compared to that measured using normal cynomolgus monkey plasma (mean ± standard deviation, n = 3).

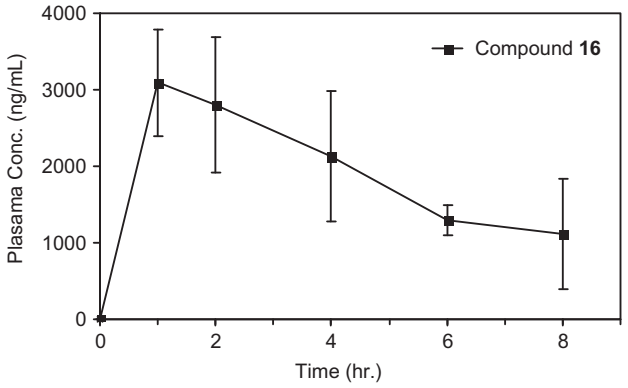

Figure 7. Plasma concentration–time profiles of compound **16** in cynomolgus monkeys after oral administration of compound **14** at a dose of 10 mg/kg (mean ± standard deviation, n = 3). Plasma concentrations of compound **14** and its sulfate conjugate were below the limit of quantification (10 ng/mL).

and introducing a potential functional group at a selected position for its bioconversion into a highly hydrophilic conjugate, using molecular modeling simulations. The phenol **14** and the corresponding glucuronide conjugate **16** showed fXa inhibitory activity comparable to that of the deshydroxy analogue **7**, which was consistent with our hypothesis that a substituent at the 3-potition of the central ring extended into the solvent sphere without interfering against inhibitor binding. Although the fXa inhibitors **7** and **16** demonstrated equivalent activity according to in vitro anticoagulant assays, pharmacodynamics of these two compounds following intravenous bolus injection resulted in remarkable differences, with the latter demonstrating 10-fold more effective in ex vivo anticoagulant assay. Pharmacokinetic data clarified the rapid transformation of the phenol **14** into the corresponding glucuronide **16** after oral dosing. These results indicated that biotransformation of compound **14** into the highly hydrophilic conjugate **16** boosted ex vivo anticoagulant activity. Compound **14** (ASP8102) was selected for advancement to further biological evaluation as an orally active antithrombotic agent.

We believe that our novel methodology is not limited to study for the discovery of fXa inhibitors. Worldwide efforts are ongoing for in the quest to identify orally active inhibitors against the coagulation cascade enzymes, such as thrombin, fXa, factor VIIa, factor VIIIa, and so on. We believe that our conjugation strategy, which selects a template compound and appropriate position for installing a trigger functional group using computer molecular modeling, will generate new orally active anticoagulants. Results of our continuing efforts to identify orally active fXa inhibitors based on this novel strategy will be published in due course.

6. Experimental section

6.1. Chemistry

^{1}H NMR spectra were recorded on a JEOL JNM-LA300 or a JEOL JNM-EX400 spectrometer and the chemical shifts are expressed in δ (ppm) values with tetramethylsilane as an internal standard (in NMR description, s = singlet, d = doublet, t = triplet, m = multiplet, and br = broad peak). Mass spectra were recorded on a JEOL JMS-LX2000 spectrometer. For salts, assignments of ion peaks are based on the basic component. The elemental analyses were performed with a Yanaco MT-5 microanalyzer (C, H, and N) and a Yokogawa IC-7000S ion chromatographic analyzer (halogens), and were within ±0.4% of theoretical values. Melting points were measured using a Yanaco MP-500D melting point apparatus without correction. C-18 reversed-phase silica gel (ODS) column chromatography was performed on YMC gel (ODS-A 120–230/70). Analytical high-performance liquid chromatography (HPLC) experiments were performed with an ODS column (Tosoh Co. TSK-GEL 80TM, i.d. = 0.46 cm, l = 15 cm). The HPLC conditions were as follows: flow rate, 1.0 mL/min; detection wavelength, 254 nm. All reagents purchased were used without further purification.

6.1.1. 3-Benzyloxy-*N*-(5-chloro-2-pyridyl)-2-nitrobenzamide (9)

To a mixture of 3-benzyloxy-2-nitrobenzoic acid (**8**)[17] (77.2 g, 283 mmol), 10 drops of *N*,*N*-dimethylformamide, and ethyl acetate (300 mL) was added thionyl chloride (101 g, 849 mmol) at ambient temperature and the whole was stirred at 50 °C for 3 h. The reaction mixture was cooled to ambient temperature and then concentrated in vacuo. The residue was dissolved in acetonitrile (200 mL). To this solution was added a solution of 2-amino-5-chloropyridine (36.4 g, 283 mmol), pyridine (22.4 g, 849 mmol) in acetonitrile (350 mL) at 0 °C and the whole was stirred at ambient temperature for 20 h. The reaction mixture was concentrated in vacuo. The residue was diluted with $CHCl_3$ (1.0 L), and washed with 1*N* hydrochloric acid, 1*N* aqueous sodium hydroxide solution, and then brine. The organic layer was dried over magnesium sulfate and concentrated in vacuo to yield the title compound as a colorless solid (98.0 g, 90%): ^{1}H NMR (300 MHz, DMSO-d_6) δ 5.35 (2H, s), 7.32–7.48 (6H, m), 7.60–7.69 (2H, m), 7.96 (1H, dd, J = 2.6 and 9.0 Hz), 8.08 (1H, d, J = 9.0 Hz), 8.45 (1H, d, J = 2.6 Hz), 11.47 (1H, s); FAB-MS (monoisotopic) m/z 384 $[M+H]^+$.

6.1.2. 2-Amino-*N*-(5-chloro-2-pyridyl)-3-hydroxybenzamide (10)

A mixture of compound **9** (98.0 g, 255 mmol), pentamethylbenzene (49.1 g, 332 mmol), and trifluoroacetic acid (250 mL) was stirred at 40 °C for 23 h. The reaction mixture was cooled to ambient temperature and then filtered. The filtrate was concentrated in vacuo. The residue was diluted with ethyl acetate (1.0 L) and washed with saturated sodium bicarbonate. The organic layer was dried over magnesium sulfate and concentrated in vacuo to yielded a colourless solid. To a mixture of this material, ethyl acetate (400 mL), and ethanol (400 mL) was added Raney® nickel in ethanol (40 mL) and the whole was stirred under hydrogen at atmospheric pressure for 29 h. To the reaction mixture was added *N*,*N*-dimethylformamide (1.2 L). The mixture was filtered through a pad of Celite® and the filtrate was concentrated in vacuo. A mixture of this material and ethyl acetate (215 mL) was stirred at 70 °C for 1 h. The resulting precipitate was filtered off and dried in vacuo to yield the title compound as a beige solid (49.5 g, 74%): ^{1}H NMR (400 MHz, DMSO-d_6) δ 5.93 (2H, s), 6.44 (1H, t, J = 8.0 Hz), 6.82 (1H, d, J = 8.0 Hz), 7.27 (1H, d, J = 8.0 Hz), 7.93 (1H, dd, J = 3.2 and 8.8 Hz), 8.14 (1H, d, J = 8.8 Hz), 8.41 (1H, d, J = 3.2 Hz), 9.60 (1H, s), 10.46 (1H, s); FAB-MS (monoisotopic) m/z 264 $[M+H]^+$.

6.1.3. 2-Amino-5-chloro-*N*-(5-chloro-2-pyridyl)-3-hydroxybenzamide (11)

A mixture of compound **10** (5.50 g, 20.9 mmol) and *N*-chlorosuccinimide (2.92 g, 21.9 mmol) in *N*,*N*-dimethylformamide (100 mL) was stirred at 50 °C for 1.5 h. Additional *N*-chlorosuccinimide (280 mg, 20.9 mmol) was added and the whole was stirred at 50 °C for 1 h. The mixture was filtered through a pad of Celite® and the filtrate was concentrated in vacuo. The residue was diluted with ethyl acetate and washed with H_2O. The organic layer was dried over magnesium sulfate and concentrated in vacuo. The residue was triturated with $CHCl_3$, filtered off, and dried in vacuo to yield the title compound as a brown solid (4.40 g, 69%): ^{1}H NMR (400 MHz, DMSO-d_6) δ 6.04(2H, br s), 6.80 (1H, s), 7.36 (1H, s), 7.93 (1H, d, J = 8.8 Hz), 8.10 (1H, d, J = 8.8 Hz), 8.42 (1H, s), 10.16 (1H, s), 10.67 (1H, s); FAB-MS (monoisotopic) m/z 298 $[M+H]^+$.

6.1.4. 2-Amino-5-bromo-*N*-(5-chloro-2-pyridyl)-3-hydroxybenzamide (12)

To a mixture of compound **10** (5.27 g, 20.0 mmol) and *N*,*N*-dimethylformamide (60 mL) was added *N*-bromosuccinimide (3.56 g, 20.0 mmol) portionwise at −15 °C and the whole was stirred for 1.5 h. Additional *N*-bromosuccinimide (356 mg, 2.00 mmol) was added at −15 °C and the whole was stirred for 2 h. To the mixture were added H_2O (120 mL) and ethyl acetate (120 mL) at −15 °C, and the whole was warm to ambient temperature and stirred for 10 min. The mixture was filtered through a pad of Celite®. The organic layer was separated, decolorized with activated charcoal, filtered through a pad of Celite®, and then concentrated in vacuo to yield the title compound as a beige solid (5.70 g, 83%): ^{1}H NMR (400 MHz, DMSO-d_6) δ 6.06 (2H, br s), 6.90 (1H, d, J = 2.0 Hz), 7.47 (1H, d, J = 2.0 Hz), 7.93 (1H, dd, J = 2.4 Hz, 8.8 Hz), 8.10 (1H, d, J = 8.8 Hz), 8.42 (1H, d, J = 2.4 Hz), 10.14 (1H, br s), 10.68 (1H, br s); FAB-MS (monoisotopic) m/z 342 $[M+H]^+$.

6.1.5. 4′-Chloro-2′-[(5-chloro-2-pyridyl)carbamoyl]-6′-hydroxyl-1-isopropylpiperidine-4-carboxanilide hydrochloride (13)

A mixture of 1-isopropylpiperidine-4-carboxylic acid (**17**)[15b] (515 mg, 3.00 mmol), 3 drops of *N*,*N*-dimethylformamide, and thionyl chloride (3.0 mL) was stirred at 80 °C for 0.5 h. The mixture was cooled to ambient temperature and concentrated in vacuo. This material was added to a mixture of compound **11** (520 mg, 1.74 mmol) and pyridine (6.0 mL) at 0 °C and the whole was stirred at ambient temperature for 12 h. The reaction mixture was concentrated in vacuo and the residue was subjected to chromatography over silica gel eluting with $CHCl_3$/MeOH/c.NH_3 (100:10:1 by volume) to yield a colourless solid (417 mg). This material was suspended in EtOH (4.0 mL). To this suspension was added 1*N* hydrochloric acid (0.4 mL) at ambient temperature and the whole was stirred for 0.5 h. The resulting precipitate was filtered off and dried in vacuo to yield the title compound as a colorless solid (308 mg, 21%): mp 249–252 °C (dec.); ^{1}H NMR (400 MHz, DMSO-d_6) δ 1.04 (1.8H, d, J = 6.3 Hz), 1.24 (4.2H, d, J = 6.3 Hz), 1.81–2.18 (4H, m), 2.63–3.26 (4H, m), 3.34–3.44 (2H, m), 7.05 (1H, s), 7.13 (1H, s), 7.91–7.96 (1H, m), 8.09–8.13 (1H, m),

8.37–8.41 (1H, m), 9.45 (0.7H, s), 9.53 (0.3H, s), 9.59 (0.7H, br s), 10.19 (0.3H, br s), 10.49–10.51 (1H, m), 10.60 (0.7H, s), 10.80 (0.3H, s); FAB-MS (monoisotopic) *m*/*z* 451 $[M+H]^+$; Anal. calcd for $C_{21}H_{24}N_4O_3Cl_2{\cdot}HCl{\cdot}0.5H_2O$: C, 50.77; H, 5.27; N, 11.28; Cl, 21.41. Found: C, 50.63; H, 5.29; N, 11.32; Cl, 21.57.

6.1.6. 4′-Bromo-2′-[(5-chloro-2-pyridyl)carbamoyl]-6′-hydroxyl-1-isopropylpiperidine-4-carboxanilide hydrochloride (14)

A mixture of compound **12** (2.39 g, 7.00 mmol), compound **17** (1.32 g, 7.70 mmol), 1-hydroxybenzotriazole hydrate (1.42 g, 10.5 mmol), 1-[3-(dimethylamino)propyl]-3-ethylcarbodiimide hydrochloride (2.02 g, 10.5 mmol). triethylamine (1.06 g, 10.5 mmol), and *N*,*N*-dimethylformamide (35 mL) was stirred at ambient temperature for 22 h. To the mixture were added H_2O (105 mL) and ethyl acetate (105 mL) at ambient temperature and the whole was stirred for 2 h. The resulting precipitate was filtered off, washed with H_2O and then ethyl acetate, and dried in vacuo to yield 1.67 g of 4′-bromo-2′-[(5-chloro-2-pyridyl)carbamoyl]-6′-hydroxyl-1-isopropylpiperidine-4-carboxanilide. This material was suspended in EtOH (60 mL). To this suspension was added 1*N* hydrochloric acid (5.0 mL) at ambient temperature and the whole was stirred for 30 h. The resulting precipitate was filtered off and dried in vacuo to yield the title compound as a colorless solid (1.35 g, 36%): mp 262–265 °C (dec.); ^{1}H NMR (400 MHz, DMSO-d_6) δ 1.04 (1.8H, d, J = 6.8 Hz), 1.24 (4.2H, d, J = 6.3 Hz), 1.74–2.12 (4H, m), 2.60–3.45 (6H, m), 7.15–7.19 (1H, m), 7.23–7.27 (1H, m), 7.89–7.97 (1H, m), 8.07–8.14 (1H, m), 8.35–8.41 (1H, m), 9.39–9.55 (1.7H, m), 9.98–10.10 (0.3H, br s), 10.44–10.50 (1H, m), 10.62 (0.7H, s), 10.81 (0.3H, s); FAB-MS (monoisotopic) *m*/*z* 495 $[M+H]^+$; Anal. calcd for $C_{21}H_{24}N_4O_3BrCl{\cdot}HCl{\cdot}0.8H_2O$: C, 46.14; H, 4.90; N, 10.25; Br, 14.62; Cl, 12.97. Found: C, 46.24; H, 4.51; N, 10.33; Br, 14.26; Cl, 13.16.

6.1.7. 5-Bromo-3-[(5-chloro-2-pyridyl)carbamoyl]-2-[(1-isopropylpiperidine-4-carbonyl)amino]phenyl β-D-glucopyranosiduronic acid trifluoroacetate (16)

To a stirred mixture of 4′-bromo-2′-[(5-chloro-2-pyridyl)carbamoyl]-6′-hydroxyl-1-isopropylpiperidine-4-carboxanilide (1.00 g, 2.02 mmol), methanol (20 mL), and $CHCl_3$ (20 mL) was added 1,8-diazabicyclo[5.4.0]undec-7-ene (921 mg, 6.05 mmol) at ambient temperature. After 30 min, to the reaction mixture was added acetobromo-α-D-glucuronic acid methyl ester (2.41 g, 6.06 mmol) at ambient temperature, and the whole was stirred for 16 h. To the reaction mixture were added sodium carbonate (1.07 g, 10.1 mmol) and H_2O (20 mL) at ambient temperature, and the whole was stirred for 23 h. The reaction mixture was concentrated in vacuo. The residue was diluted with H_2O, washed with $CHCl_3$, and then extracted with *n*-butanol. The organic layer was concentrated in vacuo. The residue was diluted with H_2O (5 mL), neutralized with acetic acid and concentrated in vacuo. The residue was subjected to chromatography over ODS gel eluting with CH_3CN/0.1% aqueous trifluoroacetic acid (4:10 by volume) to give the title compound as a colorless amorphous powder (502 mg, 28%): ^{1}H NMR (400 MHz, DMSO-d_6) δ 1.02–1.05 (1.2H, m), 1.23 (4.8H, d, J = 6.9 Hz), 1.66–2.13 (4H, m), 2.62–3.46 (9H, m), 4.02–4.05 (1H, m), 5.12 (1H, d, J = 6.8 Hz), 5.40 (3H, br s), 7.31–7.33 (1H, m), 7.38–7.40 (1H, m), 7.91–7.95 (1H, m), 8.08–8.13 (1H, m), 8.40 (0.75H, d, J = 2.5 Hz), 8.41 (0.25H, d, J = 2.5 Hz), 8.76–8.92 (1H, m), 9.46 (0.2H, s), 9.49 (0.8H, s), 10.79 (0.8H, s), 10.93 (0.2H, s), 12.88 (1H, br s); FAB-MS (monoisotopic) *m*/*z* 671 $[M+H]^+$; Anal. calcd for $C_{27}H_{32}N_4O_9BrCl{\cdot}1.7TFA{\cdot}2H_2O$: C, 40.49; H, 4.21; N, 6.21; Br, 8.86; Cl, 3.93; F, 10.94. Found: C, 40.48; H, 3.98; N, 6.30; Br, 8.72; Cl, 4.05; F, 10.68. Analytical HPLC t_R = 5.5 min, 98.6% pure (eluent; acetonitrile/0.01 M aqueous $HClO_4$ = 2:8).

6.1.8. 5-Chloro-3-[(5-chloro-2-pyridyl)carbamoyl]-2-[(1-isopropylpiperidine-4-carbonyl)amino]phenyl β-D-glucopyranosiduronic acid trifluoroacetate (15)

In a manner identical to that described above for compound **16**, from 150 mg (0.332 mmol) of 4′-bromo-2′-[(5-chloro-2-pyridyl) carbamoyl]-6′-hydroxyl-1-isopropylpiperidine-4-carboxanilide, 152 mg (1.00 mmol) of 1,8-diazabicyclo[5.4.0]undec-7-ene, 397 mg (1.00 mmol) of acetobromo-α-D-glucuronic acid methyl ester, and 114 mg (1.08 mmol) of sodium carbonate was obtained 86 mg (30%) of the title compound as a colorless amorphous powder: ^{1}H NMR (400 MHz, DMSO-d_6) δ 1.02–1.04 (1.2H, m), 1.22 (4.8H, d, J = 6.4 Hz), 1.63–2.13 (4H, m), 2.63–2.70 (1H, m), 2.86–3.14 (2H, m), 3.36–3.46 (6H, m), 4.01–4.05 (1H, m), 5.12 (1H, d, J = 6.9 Hz), 5.18–5.54 (3H, br s), 7.43–7.45 (1H, m), 7.47–7.51 (1H, m), 7.92–7.95 (1H, m), 8.08–8.14 (1H, m), 8.38–8.42 (1H, m), 8.80–9.00 (1H, br s), 9.44 (0.2H, s), 9.48 (0.8H, s), 10.79 (0.8H, s), 10.93 (0.2H, s), 12.85 (1H, br s); FAB-MS (monoisotopic) *m*/*z* 627 $[M+H]^+$; Anal. calcd for $C_{27}H_{32}N_4O_9Cl_2{\cdot}1.7TFA{\cdot}2.5H_2O$: C, 42.15; H, 4.50; N, 6.47; Cl, 8.18; F, 11.18. Found: C, 42.12; H, 4.16; N, 6.55; Cl, 8.43; F, 11.27. Analytical HPLC t_R = 5.1 min, 98.7% pure (eluent; acetonitrile/0.01 M aqueous $HClO_4$ = 2:8).

6.2. Pharmacology

6.2.1. In vitro assay for inhibition of factor Xa

The hydrolysis rates of synthetic substrates were assayed by continuously measuring absorbance at 405 nm at 37 °C with a microplate reader (model 3550, Bio-Rad, U.S.). Reaction mixtures (125 μL) were prepared in 96-wellplates containing chromogenic substrates (S-2222) and an inhibitor in either 0.05 M Tris-HCl, pH 8.4, or 0.15 M NaCl. Reactions were initiated with 25 μL of enzyme solution. The concentration of inhibitor required to inhibit enzyme activity by 50% (IC_{50}) was calculated from dose–response curves in which the logit transformation of residual activity was plotted against the logarithm of inhibitor concentration.

6.2.2. Enzyme selectivity

Reaction mixtures were prepared in 96-well plates containing the chromogenic substrate and test compound. The reaction was initiated by the addition of enzyme, and the color was continuously monitored at 405 nm using a microplate reader SpectraMax 340PC (Molecular Devices, CA, U.S.) at 37 °C. Each enzyme was used at final concentration as follows: 0.20 UmL^{-1} thrombin and 1.0 UmL^{-1} trypsin. The enzymatic activities were assessed by the amidolysis of the following chromogenic substrates for the corresponding protease: S-2222 for trypsin and S-2238 for thrombin. The rate of substrate hydrolysis (mOD min^{-1}) was measured at 37 °C. The mode of inhibition was estimated from a Lineweaver–Burk plot. The K_i was determined from a Dixon plot by plotting the reciprocal of the initial reaction velocities at different substrate concentrations against different inhibitor concentrations.

6.2.3. Prothrombin time assays in vitro

After collection of citrated blood samples from cynomolgus monkey, platelet-poor plasma was prepared by centrifugation at 3000 rpm for 10 min and stored at −40 °C until use. Plasma clotting times were measured using a KC10A coagulometer (Amelung Co., Lehbrinksweg, Germany) at 37 °C. Prothrombin time (PT) was measured using Orthobrain thromboplastin (OrthoDiagnostic Systems Co., Tokyo, Japan), and values for each test sample were compared with coagulation times of a distilled water control. The concentration required to double the clotting time (CT_2) was estimated from each individual concentration–response curve. Each measurement was performed three times and represented as the mean value.

6.2.4. Ex vivo studies

The test drug was dissolved or suspended in 10% HP-β-CyD/5% mannitol or 0.5% methyl cellulose and administered intravenously via saphenous vein or orally using a gastric tube to cynomolgus monkeys (mass range: 3.9–4.9 kg). Animals were last fed more than 12 h before drug administration. Citrated blood was collected from the femoral vein, and platelet-poor plasma was prepared by centrifugation for measurement of PT. All data were expressed as relative-fold values, compared with the baseline value of vehicle-treated cynomolgus monkeys.

6.2.5. Pharmacokinetic study

Compound **14** suspended in 0.5% methylcellulose was orally administered to male cynomolgus monkeys (mass range: 4.0–4.5 kg, HAMRI CO., Ltd or ShinNihon Sangyo, Ltd, $n = 3$) at a dose of 10 mg/kg under fasted conditions. Blood samples were collected at 1, 2, 4, 6, 8, 12, and 24 h after administration and centrifuged to obtain the plasma fraction. The plasma samples were purified by solid phase extraction using Oasis HLB 96 well plate (Waters, Japan). After extraction, the elute was evaporated to dryness, and the residue was reconstituted in mobile phase and injected into an LC–MS/MS apparatus to determine the plasma concentrations of compounds **14** and **16**. Dose and plasma concentrations were expressed as free form. Compound **13** was used as the analytical internal standard.

6.2.6. PAMPA

The PAMPA Evolution instrument from pION Inc. was used in this study. In PAMPA, a 'sandwich' is formed from a 96-well microtiter plate (pION Inc., part no. 110243) and a 96-well filter plate (Millipore, IPVH) such that each composite well is divided into two chambers: donor at the bottom and acceptor at the top, separated by a 125 μm thick microfilter disk (0.45 μm pores) and coated with a 20% (w/v) dodecane solution of a lecithin mixture (pION Inc., part no. 110669). Drug samples were introduced as 10 mM DMSO stock solutions in a 96-well polypropylene microtiter plate. The robotic liquid handling system draws a 5 μL aliquot of the DMSO stock solution and mixes it into an aqueous buffer solution including 10% (v/v) of DMSO so that the final typical sample concentration is 50 μM. The drug solutions were filtered using a 96-well filter plate (Corning, PVDF) and added to the donor compartments. The donor solutions were adjusted in pH 6.5 (NaOH-treated universal buffer, pION Inc., part no. 110151), while the acceptor solution had the same pH 7.4 (pION Inc., part no. 110139). The plate sandwich was formed and allowed to incubate at 25 °C for 2 h in a humidity-saturated atmosphere. On completion of the prescribed incubation time, the sandwich plates were separated and both the donor and acceptor compartments were assayed for the amount of material present by comparison with the UV spectrum (270–400 nm) obtained from reference standards. Mass balance was used to determine the amount of material remaining in the membrane barrier, and permeability (Pe) was calculated using PAMPA Evolution software (pION Inc.).

6.3. Computational modeling of factor Xa inhibitors

Docking simulations of factor Xa inhibitors were performed to get insight into the appropriate position for the trigger phenolic hydroxyl group, because no complex structure of factor Xa with the nonamidine-type inhibitors was available when we started this study, although some X-ray structures of factor Xa with or without amidine-type inhibitors were reported. As the X-ray structure of rat trypsin with compound **6** (PDB ID: 1QL9) was available, we started the computational molecular modeling of factor Xa and its inhibitors based on the trypsin X-ray structure. The X-ray structure of apo-form factor Xa (PDB ID: 1HCG) was selected as the model of factor Xa. The solvent molecules were removed from 1HCG so as not to prevent inhibitors from appropriate binding. Because the solvent molecules including ions in 1QL9 played an important role for reproducing the binding mode of compound **6** by docking simulations, the solvent molecules of 1QL9 were inserted into 1HCG by superposing 1QL9 over 1HCG based on the structure alignment of the two proteins. To summarize, the protein coordinates of 1HCG and the solvent coordinates of 1QL9 were used for the docking simulations. The binding pocket was defined as the cavity formed by the residues within the twice of the radius of gyration of the compound **6** in 1QL9 (10.0 angstrom) from the center of mass of the compound **6** in 1QL9. The docking program, Gold, was used for the docking simulations. The molecular visualization was produced by MOE.

Acknowledgment

The authors deeply acknowledge Drs. Shuichi Sakamoto, Tomihisa Kawasaki, and Takeshi Shigenaga for useful discussion. The authors are grateful to Ms. Yumiko Moritani for performing pharmacological experiments. The authors also thank to Dr. Takeshi Kadokura for pharmacokinetic analysis and Dr. Katsuhiro Yamano for assistance in preparing this manuscript, and the staff of the Division of Analytical & Pharmacokinetics Research Laboratories for the elemental analysis and spectral measurements.

References and notes

1. Gustafsson, D.; Nystrom, J.-E.; Carlsson, S.; Bredberg, U.; Eriksson, U.; Gyzander, E.; Elg, M.; Antonsson, T.; Hoffmann, K.-J.; Ungell, A.-L.; Sorensen, H.; Nagard, S.; Abrahamsson, A.; Bylund, R. *Thromb. Res.* **2001**, *101*, 171.
2. Hauel, N. H.; Nar, H.; Priepke, H.; Ries, U.; Stassen, J.-M.; Wienen, W. *J. Med. Chem.* **2002**, *45*, 1757.
3. Pinto, D. J. P.; Smallheer, J. M.; Cheney, D. L.; Knabb, R. M.; Wexler, R. R. *J. Med. Chem.* **2010**, *53*, 6243. and references cited therein.
4. Roehrig, S.; Straub, A.; Pohlmann, J.; Lampe, T.; Pernerstorfer, J.; Schlemmer, K. H.; Reinemer, P.; Perzborn, E. *J. Med. Chem.* **2005**, *48*, 5900.
5. Pinto, D. J. P.; Orwat, M. J.; Koch, S.; Rossi, K. A.; Alexander, R. S.; Smallwood, A.; Wong, P. C.; Rendina, A. R.; Luettgen, J. M.; Knabb, R. M.; He, K.; Xin, B.; Wexler, R. R.; Lam, P. Y. S. *J. Med. Chem.* **2005**, *50*, 5339.
6. Chung, N.; Jeon, H. K.; Lien, L. M.; Lai, W. T.; Tse, H. F.; Chung, W. S.; Lee, T. H.; Chen, S. A. *Thromb. Haemostasis* **2011**, *105*, 535.
7. Smith, D. A.; Jones, B. C.; Walker, D. K. *Med. Res. Rev.* **1996**, *16*, 243.
8. Masters, J. J.; Franciskovich, J. B.; Tinsley, J. M.; Campbell, C.; Campbell, J. B.; Craft, T. J.; Froelich, L. L.; Gifford-Moore, D. S.; Hay, L. A.; Herron, D. K.; Klimkowski, V. J.; Kurz, K. D.; Metz, J. T.; Ratz, A. M.; Shuman, R. T.; Smith, G. F.; Smith, T.; Towner, R. D.; Wiley, M. R.; Wilson, A.; Yee, Y. K. *J. Med. Chem.* **2000**, *43*, 2087.
9. Hirayama, F.; Koshio, H.; Ishihara, T.; Hachiya, S.; Sugasawa, K.; Koga, Y.; Seki, N.; Shiraki, R.; Shigenaga, T.; Iwatsuki, Y.; Moritani, Y.; Mori, K.; Kadokura, T.; Kawasaki, T.; Matsumoto, Y.; Sakamoto, S.; Tsukamoto, S. *J. Med. Chem.* **2011**, *54*, 8051.
10. The *c*log*P* values are calculated using the ACD/log*P* version 9.0 (Advanced Chemistry Development, Inc.). The sulfate conjugate of compound **1** was more lipophilic than the glucuronide conjugate **2** (*c*log*P* = 0.63).
11. (a) van Heek, M.; France, C. F.; Compton, D. S.; McLeod, R. L.; Yumibe, N. P.; Alton, K. B.; Synbertz, E. J.; Davis, H. R. *Exp. Ther.* **1997**, *283*, 157; (b) van Heek, M.; Farley, C.; Compton, D. S.; Hoos, L.; Alton, K. B.; Synbertz, E. J.; Davis, H. R. *Br. J. Pharmacol.* **2000**, *129*, 1748; (c) Kværnø, L.; Werder, M.; Hauser, H.; Carreira, E. M. *J. Med. Chem.* **2005**, *48*, 6035.
12. Ishihara, T.; Hirayama, F.; Sugasawa, K; Koga, Y.; Kadokura, T.; Shigenaga, T. (Yamanouchi Pharmaceutical Co., Ltd, Japan). PCT Int. Appl. WO2002042270, 2002.
13. Pinto, D. J. P.; Orwat, M. J.; Wang, S.; Fevig, J. M.; Quan, M. L.; Amparo, E.; Cacciola, J.; Rossi, K. A.; Alexander, R. S.; Smallwood, A. M.; Luettgen, J. M.; Liang, L.; Aungst, B. J.; Wright, M. R.; Knabb, R. M.; Wong, P. C.; Wexler, R. R.; Lam, P. Y. S. *J. Med. Chem.* **2001**, *44*, 566.
14. Faull, A. W.; Mayo, C. M.; Preston, J; Stocker, A. (Zeneca Limited, UK). PCT Int. Appl. WO9610022, 1996.
15. (a) Kyle, J. A.; Bailey, B. D.; Buben, J.; Chirgadze, N. Y.; Chouinard, M.; Craft, T. J.; Daniels, W. D.; Denny, C. P.; Ficorilli, J.; Franciskovich, J. B.; Froelich, L. L.; Gifford-Moore, D. S.; Goodson, T.; Halligan, N. G.; Hay, L.; Herron, D. K.; Jackson, C. V.; Joseph, S. P.; Klimlowski, V. J.; Kurz, K. D.; Linebarger, J. H.; Masters, J. J.; McCowan, J. R.; Mendel, D.; Muegge, L. P.; Murphy, A. T.; Pineiro-Nunez, M. M.; Ratz, A. M.; Shetler, T. J.; Smallwood, J. K.; Smith, G. F.; Tinsley, J. M.; Towner, R. D.; Trankle, W. G.; Waid, P.; Weir, L. C.; Yee, Y. K.; Wiley, M. R. Presented at the 220th National Meeting of the American Chemical Society,

Washington, D.C., Aug 20–24, 2000, MEDI–288.; (b) Beight, D. W.; Craft, T. J.; Denny, C. P.; Franciskovich, J. B.; Goodson, T.; Hall, S. E.; Herron, D. K.; Joseph, S. P.; Klimlowski, V. J.; Masters, J. J.; Mendel, D.; Milot, G.; Pineiro-Nunez, M. M.; Sawyer, J. S.; Shuman, R. T.; Smith, G. F.; Tebbe, A. L.; Tinsley, J. M.; Weir, L. C.; Wikel, J. H.; Wiley, M. R.; Yee, Y. K.; (Eli Lilly Co., USA). PCT Int. Appl. WO0039118, 2000.

16. (a) Holloway, C. J.; Zierhut, M. *IRCS Med. Sci.: Libra. Compend.* **1981**, *9*, 96; (b) Kim, K. H. *J. Pharm. Sci.* **1991**, *80*, 966; (c) Ebner, T.; Burchell, B. *Drug Metab. Dispos.* **1993**, *21*, 50.
17. Zymalkowski, F.; Happel, K. H. *Chem. Ber.* **1969**, *102*, 2959.
18. (a) Schmidt, R. R.; Grundler, G. *Synthesis* **1981**, 885; (b) Badman, G. T.; Green, D. V. S.; Voyle, M. *J. Organomet. Chem.* **1990**, *388*, 117; (c) Berrang, B.; Brine, G. A.; Carrol, F. I. *Synthesis* **1997**, 1165.